Electric-Analog Studies of Brine Coning Beneath Fresh-Water Wells in the Punjab Region, West Pakistan

GEOLOGICAL SURVEY WATER-SUPPLY PAPER 1608–J

Prepared in cooperation with the West Pakistan Water and Power Development Authority, under the auspices of the U.S. Agency for International Development

Electric-Analog Studies of Brine Coning Beneath Fresh-Water Wells in the Punjab Region, West Pakistan

By G. D. BENNETT, M. J. MUNDORFF, *and* S. AMJAD HUSSAIN

CONTRIBUTIONS TO THE HYDROLOGY OF ASIA AND OCEANIA

GEOLOGICAL SURVEY WATER-SUPPLY PAPER 1608-J

Prepared in cooperation with the West Pakistan Water and Power Development Authority, under the auspices of the U.S. Agency for International Development

UNITED STATES GOVERNMENT PRINTING OFFICE, WASHINGTON : 1968

UNITED STATES DEPARTMENT OF THE INTERIOR

STEWART L. UDALL, *Secretary*

GEOLOGICAL SURVEY

William T. Pecora, *Director*

For sale by the Superintendent of Documents, U.S. Government Printing Office
Washington, D.C. 20402 - Price 55 cents (paper cover)

CONTENTS

ILLUSTRATIONS

TABLE

CONTRIBUTIONS TO THE HYDROLOGY OF ASIA AND OCEANIA

ELECTRIC-ANALOG STUDIES OF BRINE CONING BENEATH FRESH-WATER WELLS IN THE PUNJAB REGION, WEST PAKISTAN

By G. D. BENNETT, M. J. MUNDORFF, and S. AMJAD HUSSAIN

ABSTRACT

A graphical procedure developed by Morris Muskat to deal with the problem of water coning beneath an oil well was utilized to study the coning of brine or brackish water beneath a fresh-water well, supplied at equilibrium by uniform areal recharge. The fresh-water head distributions employed in this technique were obtained from an analog model for steady-state axisymmetrical flow to a well, of the type described by Stallman (1963). This model was equipped with a system of switches by means of which resistors could be removed from the lower part of the network to simulate the truncation of the zone of fresh water by the brine cone.

Through a technique of successive approximation, the lower boundary of the model was adjusted to simulate the highest stable position of the brine cone in each of 18 different experiments. Flownets corresponding to this condition of highest stable coning were constructed from the analog results for each experiment. The series of experiments represented six screen penetrations at each of three values of the parameter $\frac{(h_0)^2}{r_e}\frac{K_l}{K_z}$, where h_0 is the thickness of fresh water at the radius of influence, r_e, of the well; K_l is the lateral permeability; and K_z the vertical permeability. Dimensionless functions, yielding the drawdown and discharge of the well when the brine cone is in its highest stable position, were calculated from the results of each experiment, and the variations of these functions with screen penetration and with $\frac{(h_0)^2}{r_e}\frac{K_l}{K_z}$ were studied.

Applied to conditions in the Punjab Region of West Pakistan, the results indicate that prospects are good for the development of wells capable of yielding fresh water above a stable cone in the underlying brine or brackish water.

INTRODUCTION

PURPOSE AND SCOPE OF REPORT

The Punjab Region of West Pakistan consists of a vast alluvial plain underlain by an unconfined aquifer, in which fresh water in

many places lies above more dense brackish water or brine. In the plans for ground-water development in the Punjab Region, considerable attention has been given to the problem of contamination of partially penetrating fresh-water wells by upward flow of poor-quality water from below the well. Initially, interest was focused on areas where the fresh-water layer was relatively thin. For these areas, shallow wells, termed "skimming wells," were proposed, the function of which was to discharge fresh water at equilibrium above a stable cone in the fresh water-brine interface. More recently, questions have arisen regarding the possibility of contamination of fresh-water wells 200–300 feet deep, in areas where the transition to brine is several hundred feet below the surface. These deeper wells should evidently also be operated so at to discharge fresh water above a stable brine cone, if contamination is to be completely avoided.

The problem is similar to that of water coning beneath an oil well. In this paper, a graphical procedure suggested by Muskat (1937, p. 487–490; 1949, p. 226–236) for the latter problem is adapted to the coning of brine beneath water wells. In applying this graphical procedure, Muskat employed certain analytic expressions for the potential distribution about a partially penetrating well in an aquifer of uniform thickness and used, in addition, the results of experiments on a pressed carbon electric analog. In the work herein described, the required potential distributions were obtained through an analog model made up of a network of electrical resistances, as described by Stallman (1963, p. H206–H218). The model used in this study, moreover, was equipped with a system of switches by which the lower boundary of the network could be adjusted to simulate the truncation of the fresh-water zone by the brine cone. Thus, it was possible to utilize trial-and-error methods to obtain a lower boundary which satisfied the brine-interface relations in each case. In using analytic expressions, on the other hand, Muskat found it necessary to assume that the potential distribution in the fresh water, as given by these expressions, was unaffected by the coning. Other advantages of the analog technique were that it permitted a convenient method for treating a wide variety of well penetration and anisotropy-dimension combinations, and that it permitted a closer simulation of the boundary conditions generally prevailing in the field than would have been possible with the available analytic expressions.

In using Muskat's procedure to study the coning of brine into fresh water, the effects of diffusion and dispersion must be neglected. This simplification places certain restrictions on the utility of the results. Nevertheless, as a first approximation, the method appears to have considerable value.

Cylindrical coordinates are used in the discussions in this paper. It is assumed that the brine is static, and that steady-state axisymmetrical flow to a well coaxial with the z axis occurs in the overlying fresh water.

Because the analysis is limited to steady-state conditions of flow, no information is provided regarding the time it will take for the brine interface to reach a certain position. All references to the interface position, moreover, describe its condition during pumping, rather than prior to pumping. Thus, the thickness of fresh water prior to pumping does not, strictly speaking, appear anywhere in the analysis. However, the thickness of fresh water prior to pumping may generally be considered equal to the thickness of fresh water at the radius of influence of the discharging well during pumping. It is assumed, in the analyses herein made, that the interface is virtually horizontal over the area of influence of the well prior to pumping.

The level of the interface, during pumping, at the radius of influence of the well is taken as the datum for elevation and hydraulic head. If the water table at the radius of influence stands at a level h_0 above this datum, then h_0 is both the thickness of fresh water at the radius of influence and the hydraulic head on the water table at the radius of influence. The elevation, z, of any point above the datum may be indicated in a convenient dimensionless form as $\frac{z}{h_0}$. Similarly, if r_e is used to represent the radius of influence of the well, the radial coordinate of any point may be expressed in a convenient dimensionless form as $\frac{r}{r_e}$. Finally, the hydraulic head, h, at a point may be exressed in the dimensionless form, $\frac{h-h_w}{h_0-h_w}$, where h_w is the head along the well screen. If the level of the water table prior to pumping is assumed equal to h_0, then h_0-h_w is simply the drawdown of the pumping well, neglecting entrance loss. These various dimensionless forms will be found useful in giving generality to the analog results, as well as in carrying out the graphical procedure of Muskat.

ACKNOWLEDGMENTS

The work reported in this paper was performed as part of the general program of gound-water investigations being carried out by the Water and Soils Investigations Division (WASID), West Pakistan Water and Power Development Authority (WAPDA), under the supervision of Mr. S. M. Said, Chief Engineer. The authors are indebted to Mr. Said and to Mr. M. A. Lateef, formerly Superintending Engineer, General Hydrology Circle, WASID, for their unfailing cooperation and support in all matters relating to the study. Credit is due to

Messrs. Amir-ud-Din Qureshi, M. Hasan Mian, A. A. Sehgal and K. F. Sheikh, all of the General Hydrology Circle, WASID, for their assistance in building the analog model and performing the experiments. The authors are indebted to Mr. D. M. Milne, of Sir M. MacDonald and Partners, London, for several helpful discussions relating to the techniques used in the study.

DENSITY INTERFACE RELATIONS

The mechanics of fluid density interfaces has received extensive attention in the literature (see, for example, Hubbert, 1940). If the fresh-water head on the brine interface at the radius of influence of the discharging well $\left(\text{that is, at the point } \frac{r}{r_e}=1, \frac{z}{h_o}=0\right)$ is denoted h', and if the brine is assumed to be static, it can readily be demonstrated that fresh-water heads along the interface must obey the equation

$$h=h'-\frac{\Delta\rho}{\rho_f}z, \tag{1}$$

where z is the elevation, $\Delta\rho$ is the density difference, or brine density minus fresh-water density, and ρ_f is the fresh-water density. If vertical components of flow were negligible at r_e, h' would be virtually equal to h_0. However, the condition of uniform vertical recharge usually produces measurable vertical head differences at r_e, so that the head on the interface at this radius will be less than h_0. Equation 1 applies within the brine region as well as along the interface. Using the dimensionless expressions for elevation and head, equation 1 becomes

$$\frac{h-h_w}{h_0-h_w}=\frac{h'-h_w}{h_0-h_w}-\left[\frac{\Delta\rho}{\rho_f}\cdot\frac{h_0}{h_0-h_w}\right]\frac{z}{h_0}. \tag{2}$$

EQUATIONS OF FLOW

The equation for steady-state axisymmetrical flow to a partially penetrating well in a homogeneous aquifer, exhibiting simple two-directional anisotropy, may be stated as follows:

$$K_l\left[\frac{\partial^2 h}{\partial r^2}+\frac{1}{r}\frac{\partial h}{\partial r}\right]+K_z\frac{\partial^2 h}{\partial z^2}=0, \tag{3}$$

where

K_l is the lateral permeability,
K_z is the vertical permeability,
h is the hydraulic head,
r and z are the cylindrical coordinates.

The solution to a given problem of flow to a partially penetrating well consists of a solution to the differential equation 3 for the applicable boundary conditions. In the brine-coning studies herein reported, these boundary conditions were fixed by the assumptions made regarding the flow system around the well. The assumption of steady-state flow, for example, fixes the head at a constant value, h_w, along the well screen. It was assumed that drawdowns along the water table were a small fraction of the thickness of fresh water throughout the system. This assumption implies that the reduction in thickness of flow due to the depression in the free surface is negligible compared to the reduction in thickness due to the coning of brine, and that the water table may be considered in effect a horizontal plane. It was also assumed that the steady-state flow was sustained by a constant vertical recharge applied uniformly to the water table over the area of influence of the well. This condition implies that the vertical component of head gradient at the free surface is constant over the area of influence of the well, and is given by

$$\left(\frac{\partial h}{\partial z}\right)_f = \frac{Q}{K_z \pi r_e^2}, \tag{4}$$

where $\left(\frac{\partial h}{\partial z}\right)_f$ is the vertical component of head gradient at the free surface, Q is the constant discharge of the well, and the other terms are as previously defined. Another assumption was that the head on the water table at the radius r_e during pumping was virtually equal to the head throughout the fresh water prior to pumping. As noted above, the difference in head, $h_0 - h_w$, between the water table at r_e and the screen will then be equal to the drawdown of the pumping well. In each individual flow problem, finally, boundary conditions were imposed by the assumed geometry of the well screen in relation to the aquifer. As the well screen was considered a cylinder coaxial with the z axis, its geometry could be fully described by three quantities: the fractional elevations of its upper and lower extremities, designated $\frac{z_t}{h_0}$ and $\frac{z_b}{h_0}$, respectively, and the fractional screen radius, $\frac{r_w}{r_e}$.

The assumptions and boundary conditions outlined above might be approximated, for example, around a well in the interior of an extensive well field, in which pumpage is controlled to balance vertical recharge within the field area. In any case, it seems difficult to vary the assumptions appreciably without bringing excessive complications into the analysis. If the system is not assumed to be in equilibrium, for example, the interface itself must be considered in motion, and no analysis aimed at determining a stable interface position can have meaning.

306-887 O - 68 - 2

ANALOG MODEL

The analog model used in the coning studies was of the type described by Stallman (1963). In this type of model, a two-dimensional network of resistors is used to represent the $r-z$ plane in the axisymmetrical flow system. In the aquifer, the resistance to both lateral and vertical flow decreases with increasing radial distance from the z axis, owing to increasing areas of flow. These effects are simulated in the model by varying the value of resistance used in successive vertical rows, while using a constant value of resistance and a logarithmic scale of distance along the lateral rows. Resistances along the model borders are increased, according to appropriate design formulas, to account for the smaller segments of aquifer represented by these boundary rows.

The model used in the brine-coning studies was equipped with cut-off switches and auxiliary switch-controlled resistors at each junction in the lower half of the network. By means of these components, resistors could be switched out of the lower part of the network in any required pattern; while, at the same time, resistances along the new boundaries of the network, thus established, could be increased to the proper boundary values. Thus, it was unnecessary to dismantle or rebuild the network during the trial-and-error solution procedure, for all the required adjustments of the lower boundary were effected by manipulation of the switches.

If the aquifer is free from heterogeneity, and if the flow system is of constant thickness, m, rather than of varying thickness as in the brine-coning problem, it is readily shown that a given model network can represent any aquifer for which the term $\left(\frac{m}{r_e}\right)^2 \frac{K_l}{K_z}$ has a particular value, and for which the constants $\frac{z_t}{h_0}$, $\frac{z_b}{h_0}$, and $\frac{r_w}{r_e}$ remain the same. In the brine-coning problem, where the thickness of flow varies with radial distance, it can similarly be shown that a given model can represent any system for which the term $\left(\frac{h_0}{r_e}\right)^2 \frac{K_l}{K_z}$ has a particular value, again provided the screen geometry is the same in each of these systems. The term $\left(\frac{h_0}{r_e}\right)^2 \frac{K_l}{K_z}$ will be referred to in this paper as the "flownet constant." An analog experiment performed on a model network having a flownet constant of 0.04 could represent conditions in an isotropic aquifer in which r_e were 2,500 feet and h_0 (the thickness of fresh water at r_e) were 500 feet; or it could represent conditions in an aquifer in which $\frac{K_l}{K_z}$ were 4, r_e were

1,000 feet, and h_0 were 100 feet; or so on. The experimental results herein quoted are given in dimensionless form for various values of the flownet constant. The basic analog unit built for the brine-coning studies was designed so that different values of the flownet constant could be obtained by making relatively minor changes in the model, that is, by adding vertical rows at one side of the network and removing them from the other. Flownet constants of 1.71, 0.423, and 0.0256 were represented in the experiments performed in this study.

When set for a uniform thickness of flow, the networks used in the brine-coning experiments always contained 11 lateral rows. Of these, the upper and lowermost were boundary rows, each representing a thickness of 0.05 h_0, whereas the remaining nine were internal rows, each representing a thickness of 0.1 h_0. In the switching process, therefore, it was possible to reduce the thickness of flow in stepwise increments each equal to 0.1 h_0.

The model was designed so that in the inner part of the network (toward r_w), the radius represented by each junction was twice that represented by the next junction inward; whereas in the outer part of the model (toward r_e), the radius represented by each junction was $\sqrt{2}$ times that represented by the next junction inward. The transition between these two network spacings appeared at a new position in the network each time the model was altered to represent a new value of the flownet constant; because of this, and because the ratio of r_w to r_e was kept the same in all experiments, the total number of vertical rows in the model was different for the different values of the flownet constant. No resistance above 36 megohms was used in the model; where the design formulas indicated that a higher value of resistance was required in a vertical row, the vertical connections in that row were left open. The networks representing a flownet constant of 1.71 thus contained 16 vertical rows, the inner two of which were open, with the transition in network spacing occurring at the ninth row, numbering from the screen row as one. The networks representing a flownet constant of 0.423 contained 17 vertical rows, the innermost one of which was open, with the transition in network spacing occurring at the eighth row. The networks representing a flownet constant of 0.0256 contained 19 vertical rows, none of which were open, with the transition in network spacing occurring at the sixth row. Errors caused by leaving vertical connections open in the inner rows are believed negligible, inasmuch as the current in vertical resistors of more than 10 megohms resistance was observed to be negligible throughout the series of experiments.

EXPERIMENTAL TECHNIQUE AND GRAPHICAL ANALYSIS

The model experiments were performed with the help of an analog-model analyzer of the type developed by the Water Resources Division of the U.S. Geological Survey. Through the familiar analogy between steady-state electric flow and steady-state flow of liquid through porous media, voltage measurements made at the junctions of the analog network may be used to construct a finite-difference solution to equation 3, if the electric boundary conditions imposed upon the model conform to the hydraulic boundary conditions in the problem of interest. The condition of uniform recharge per unit area was simulated by introducing current at selected junctions along the upper side of the model, in amounts proportional to the surface area of aquifer represented by the segments of the model network to either side of each selected junction. The well screen was simulated by a wire connecting the appropriate junctions at r_w, and connected in turn to the ground terminal of the analyzer.

In the early experiments, the model network was initially set up to represent an aquifer of uniform thickness. The screen and recharge connections were fixed in the required positions, and the recharge currents adjusted to the required values. Voltage measurements were then made at significant points of the analog network, and the voltage readings were converted to values of fractional head using the relation

$$\frac{\Phi}{\Phi_m}=\frac{h-h_w}{h_0-h_w}, \tag{5}$$

where Φ is the voltage at any point in the model, measured above the screen voltage as zero; Φ_m is the maximum voltage in the model—that is, the voltage at the junction $\left(\frac{r}{r_e}=1, \frac{z}{h_0}=1\right)$, again above the screen voltage as zero; and the other terms are as previously defined.

Following the calculation of fractional heads at the required junction points, a graphical analysis similar to that described by Muskat (1937, p. 487–490) was employed to determine the maximum stable interface elevation below the well. This initial analysis was made assuming that the head values obtained for the aquifer of uniform thickness would remain unchanged in the presence of the interface boundary. When the approximate interface position was located by Muskat's technique, the model network was terminated along this approximate interface boundary, new potential readings were taken, and the graphical procedure was repeated. The network was then terminated along the new interface position obtained in the second graphical approximation, and a third analysis was made, and so on, until the boundary of the

model and the interface position indicated by the graphical procedures were in close agreement. Generally, it was found that no more than one or two repetitions of the graphical procedure were required in any one case; and in some of the later experiments it was found possible to dispense with the initial analysis using the model of uniform thickness and to proceed directly with the network terminated along an approximate interface position. (In all experiments, however, readings were taken for a model of uniform thickness before concluding the experiment, for purposes of comparison with the final results.) In the following paragraphs the experimental and analytical procedure will be described as it was followed in the early experiments. The initial graphical analysis, based upon the model of uniform thickness, will first be considered in detail; following this, the procedure of successive approximation will be described.

The values of fractional head determined in the initial model experiment along the ordinate at r_w, vertically below the well, were first plotted against the corresponding values of $\frac{z}{h_0}$. In all cases the result was a curve of the general shape shown in figure 1. The value of $\frac{h-h_w}{h_0-h_w}$ at the point $\left(\frac{r}{r_0}=1, \frac{z}{h_0}=0\right)$ was then marked on the ordinate of the plot, as the intercept point $\frac{z}{h_0}=0, \frac{h-h_w}{h_0-h_w}=\frac{h'-h_w}{h_0-h_w}$ on figure 1. A line was drawn tangent to the curve from this intercept point, as indicated by the solid straight line of figure 1. This line is actually a graph of equation 2 for one particular value of the slope, $\frac{\Delta\rho}{\rho_f}\cdot\frac{h_0}{h_0-h_w}$. Its intersection, or point of tangency, with the curve of fractional head values from the flownet marks the highest point, directly beneath the well, at which the initial solution to the flow equation 3, and an equation of the form of equation 2 can both be satisfied, while at the same time the brine interface is hydrodynamically stable.

The lower dashed line in figure 1, it may be noted, has two points of intersection with the curve of fractional head values from the flownet; this lower line is of course also a graph of equation 2, though for a different value of slope. The first intersection of this line with the curve occurs at $\frac{z}{h_0}=0.14$. At this position, both equations are satisfied, and the brine interface could exist at this elevation beneath the well. At the second intersection, at $\frac{z}{h_0}=0.63$, both equations are again satisfied; however, as pointed out by Muskat, the interface cannot be hydrodynamically stable at this higher intersection. The slope of the

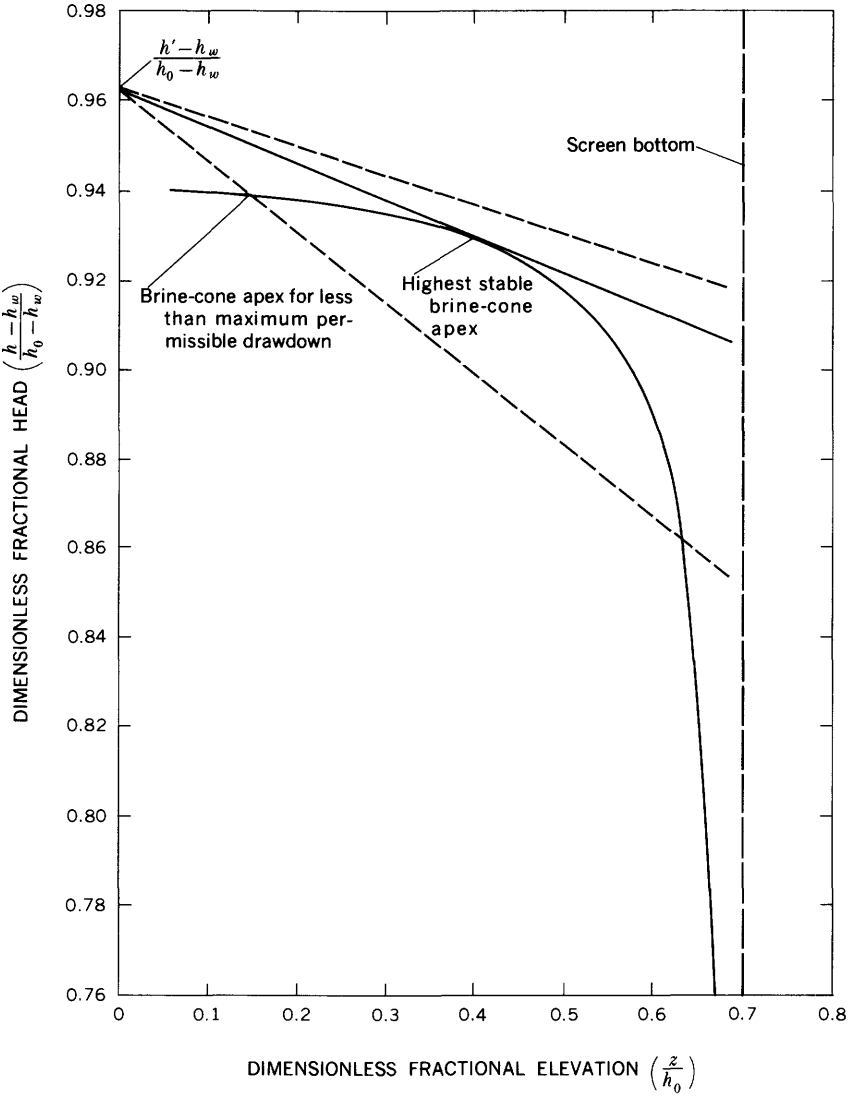

FIGURE 1.—Typical graph of $\frac{h-h_w}{h_0-h_w}$ versus $\frac{z}{h_0}$ along vertical beneath the well screen, with lines representing the interface equation for various values of $\frac{\Delta\rho}{\rho_f}\cdot\frac{h_0}{h_0-h_w}$.

curve is greater than that of the line at this point, indicating that the vertical gradient of fresh-water head above the interface is greater than that within the brine, at this elevation. This, in turn, indicates that if a particle of brine were placed within the fresh water at this point (assuming, for purposes of discussion, that it could maintain its identity as a discrete fluid particle within the fresh water), the upward

pressure force on the brine particle would exceed the downward gravitational force, in spite of the greater density of the brine, and the particle of brine would move upward toward the well. In contrast, if a particle of brine were placed within the fresh water at the elevation of the lower intersection, the downward gravitational force on the brine would exceed the upward pressure force, and the particle of brine would move downward toward the interface. Thus, while either intersection marks an elevation at which both equations are satisfied, only the lower marks a stable interface position. If the interface were at the elevation marked by the upper intersection, any slight perturbation of the interface would cause brine to enter the well. The tangent point of the solid line with the curve thus marks the highest stable position of the brine-cone apex.

The upper dashed line in figure 1 represents a graph of equation 2 for a third value of slope. At this slope, however, there is no intersection with the curve of fractional heads from the well flownet. Thus, if the term $\frac{\Delta\rho}{\rho_f}\cdot\frac{h_0}{h_0-h_w}$ is less than 0.081, the slope of the tangent line in figure 1, there can be no stable interface beneath the particular well represented by the figure. This implies, since the terms $\frac{\Delta\rho}{\rho_f}$ and h_0 are fixed for a given situation, that there is a maximum drawdown for each situation which must not be exceeded if inflow of brine is to be avoided. Associated with this maximum permissible drawdown, according to the specific capacity of the well, there is a maximum permissible discharge which cannot be exceeded without contamination.

In the brine-coning studies herein reported, attention was concentrated on the maximum stable interface elevation in each case. Thus, the tangent line of figure 1, rather than one of the lines having two intersections with the curve, was constructed in every case. The point of tangency gives the fractional elevation of the highest stable apex of the cone, directly beneath the well. All other points on the brine interface, for this case of maximum stable-cone elevation, must exhibit fresh-water heads and elevations which satisfy the equation of the tangent line. Thus, when the initial tangent line was constructed, the fractional heads were noted along each horizontal row of the model, beginning with the lowermost; and resistors were switched out of the lower part of the model in such a way that the elevations and heads of the points along the lower boundary approximately satisfied the tangent line. At the same time, the resistors along the new lower boundary were increased according to the appropriate design criteria by switching auxiliary resistors into series with the original components. The model experiment was then rerun, noting values of fractional head in the lower part of the model,

and the graphical procedure was repeated. This second graphical analysis generally resulted in a slightly different curve of fractional heads versus elevation for the vertical beneath the well, and thus in a slightly altered tangent line. At the same time, the values of fractional head along the lower boundary were slightly altered. If the heads and elevations along the boundary failed to conform to the new tangent line, the boundary was readjusted by manipulation of the switches, and the procedure repeated, until a tangent line and lower boundary in conformity with one another were obtained. The model was then taken as representative of the fresh-water flow system under conditions of maximum stable coning, and readings were taken throughout the ntework to establish the final flownet.

A dimensionless specific-capacity function, $\frac{Q}{h_0 K_l (h_0 - h_w)}$, can be calculated from the experimental results. The discharge of a well is given by

$$Q = 2\pi K_l \int_{z_b}^{z_t} \left(\frac{\partial h}{\partial \ln r}\right)_w dz, \tag{6}$$

where $\left(\frac{\partial h}{\partial \ln r}\right)_w$ is the derivative of head with respect to the natural logarithm of radial distance, evaluated at r_w, and the other terms are as previously defined. Equation 6 is obtained by applying Darcy's Law at the well face. The integral in equation 6 was evaluated by numerical approximation using the analog results. The model, as already noted, was constructed so that in the inner part of the network (toward r_w), the radius represented by each junction was twice that represented by the next junction inward. Each resistor connected to the screen terminal thus represented a segment of aquifer extending from r_w to $2r_w$, and having a vertical thickness, Δz, equal to $\frac{h_0}{10}$. If Φ_2 represents the potential at the outer end of one of these resistors and h_2 the corresponding head in the aquifer, the head drop across the segment of aquifer represented by the resistor is given by equation 5 as

$$h_2 - h_w = \frac{\Phi_2}{\Phi_m}(h_0 - h_w). \tag{7}$$

For an experiment in which n resistors are connected to the screen, the integral in equation 6 can be evaluated approximately as

$$\int_{z_b}^{z_t} \left(\frac{\partial h}{\partial \ln r}\right)_w dz = \sum_{i=1}^{n} \frac{h_{2i} - h_w}{\Delta \ln r} \cdot \Delta z = \sum_{i=1}^{n} \frac{\frac{\Phi_{2i}}{\Phi_m}(h_0 - h_w)}{\ln 2} \cdot \frac{h_0}{10}. \tag{8}$$

In equation 8, all the terms except Φ_{2i} can be placed outside the summation. Thus, the expression for well discharge, obtained by substitution into equation 6, is

$$Q=\frac{2\pi h_0 K_l(h_0-h_w)}{\Phi_m\ 10\ \ln 2}\cdot\sum_{i=1}^{n}\Phi_{2i}. \tag{9}$$

Combining the constants and transposing to obtain the dimensionless specific-capacity term gives, approximately,

$$\frac{Q}{h_0K_l(h_0-h_w)}=\frac{0.91}{\Phi_m}\sum_{i=1}^{n}\Phi_{2i}. \tag{10}$$

Using equation 10, values of the dimensionless specific-capacity term were calculated for each experiment. This function is of interest in that it permits calculation of the well discharge associated with a given brine-coning situation.

RESULTS

Eighteen experiments were performed during the course of the study. Of these, six represented a flownet constant, $\left(\frac{h_0}{r_e}\right)^2\frac{K_l}{K_z}$, of 1.71, six represented a flownet constant of 0.423, and six represented a flownet constant of 0.0256. In all the experiments, the ratio of screen radius to radius of influence $\frac{r_w}{r_e}$, was taken as 1/2896, and the top of the screen was set at $\frac{z}{h_0}$=0.95. The position of the screen bottom was set at $\frac{z}{h_0}$=0.35, 0.45, 0.55, 0.65, 0.75, and 0.85, respectively, in the six experiments performed at each flownet constant.

Plate 1 shows the final flownets obtained in each experiment. In these flownets, the solid lines represent streamlines, or the intersections of three-dimensional stream surfaces with the r–z plane. The streamlines are marked with appropriate values of the stream function, ψ, indicating the fraction of the well discharge enclosed by the particular stream surface. In each flownet, the streamline ψ=1.0 extends along the vertical at $\frac{r}{r_e}$=1.0, then follows the brine interface, and extends upward along the vertical beneath the screen. The streamline ψ=0 follows the vertical between the water table and the top of the screen. The dashed lines represent lines of equal head, or the intersections of surfaces of equal head with the r–z plane, and are numbered according to the value of $\frac{h-h_w}{h_0-h_w}$ along the surface in question. In each flownet

the lines for $\frac{h-h_w}{h_0-h_w}$ equal to 0.5, 0.7, 0.8, and 0.9 have been drawn; the lines representing lower heads fell in a virtually logarithmic pattern with respect to radial distance, in the interval between the well screen and the 0.5 line. The value of $\frac{h'-h_w}{h_0-h_w}$—that is, the value of $\frac{h-h_w}{h_0-h_w}$ at $\frac{r}{r_e}=1.0$, $\frac{z}{h_0}=0$—has been marked on each flownet. In constructing the flownets of the figures on plate 1, the ratio $\frac{h_0}{r_e}$ was taken as 0.173. Thus, as constructed, the figures for experiments A–1—A–6 correspond to an anisotropy, $\frac{K_l}{K_z}$, of about 60 to 1, those for B–1—B–6 correspond to an anisotropy of about 15 to 1, and those for C–1—C–6 correspond to an anisotropy of about 0.9 to 1. However, each figure can be replotted in true scale for any desired ratio of $\frac{h_0}{r_e}$ or $\frac{K_l}{K_z}$, so long as the flownet constant, $\left(\frac{h_0}{r_e}\right)^2\frac{K_l}{K_z}$, retains its indicated value.

It should be kept in mind that the flownets of the figures on plate 1 represent the condition of maximum stable coning and thus of maximum flow, for each situation. If the well in experiment A–1, for example, were operated at less than the maximum permissible drawdown and discharge, the interface would be lower than that shown in the illustration, and the flownet would differ somewhat from the one shown. Moreover, the interface shown in the figure is the highest possible stable interface position for the particular screen geometry and flownet constant represented in the experiment (and for the condition of uniform recharge over the area of influence), regardless of the density contrast, $\frac{\Delta\rho}{\rho_f}$, between the two fluids. As indicated in equation 2, it is the product $\frac{\Delta\rho}{\rho_f}\cdot\frac{h_0}{h_0-h_w}$, rather than the density contrast alone, which enters into determination of the interface elevation. The flownet and interface of the figure could apply equally to a system in which the density contrast, $\frac{\Delta\rho}{\rho_f}$, were 0.01, or to a system in which this contrast were 0.1; the difference is that the drawdown and discharge associated with the highest stable interface would be correspondingly greater for the higher density contrast.

Figures 2 through 6 show plots of the fractional potential, $\frac{h-h_w}{h_0-h_w}$, versus $\frac{z}{h_0}$, for the vertical below the well, for five selected experiments.

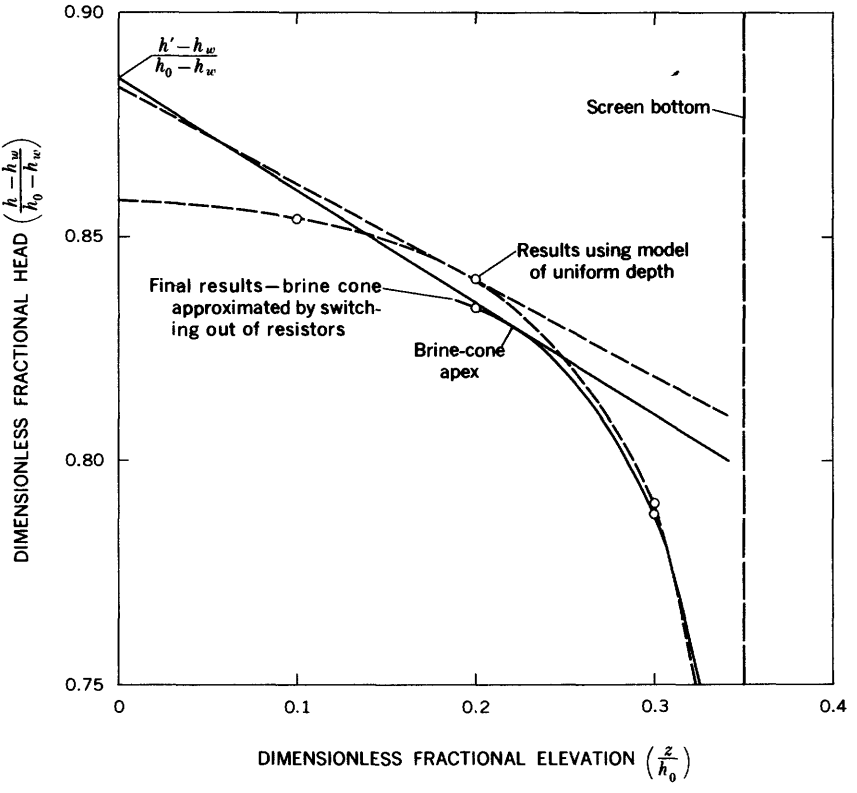

FIGURE 2.—Graph of $\frac{h-h_w}{h_0-h_w}$ versus $\frac{z}{h_0}$ at $\frac{r}{r_e}=\frac{r_w}{r_e}$, and tangent line, experiment A–1.

The tangent line drawn from the intercept point, $\left(0, \frac{h'-h_w}{h_0-h_w}\right)$, is also shown on each plot. The solid curve and tangent line in each illustration represent the final results, obtained with the lower boundary of the model adjusted to the interface position. The dashed curve and tangent line represent the initial results, taken with the model adjusted to uniform thickness.

The results of the 18 experiments are summarized in table 1. This table gives the experiment number, the flownet constant, the fractional elevation of the screen bottom, the fractional elevation of the apex of the highest stable brine cone, the slope, $\frac{\Delta\rho}{\rho_f}\cdot\frac{h_0}{h_0-h_w}$, of the (tangent) line representing the interface equation, the value $\frac{h'-h_w}{h_0-h_w}$, and the dimensionless specific-capacity term, $\frac{Q}{h_0K_i(h_0-h_w)}$, for each experiment.

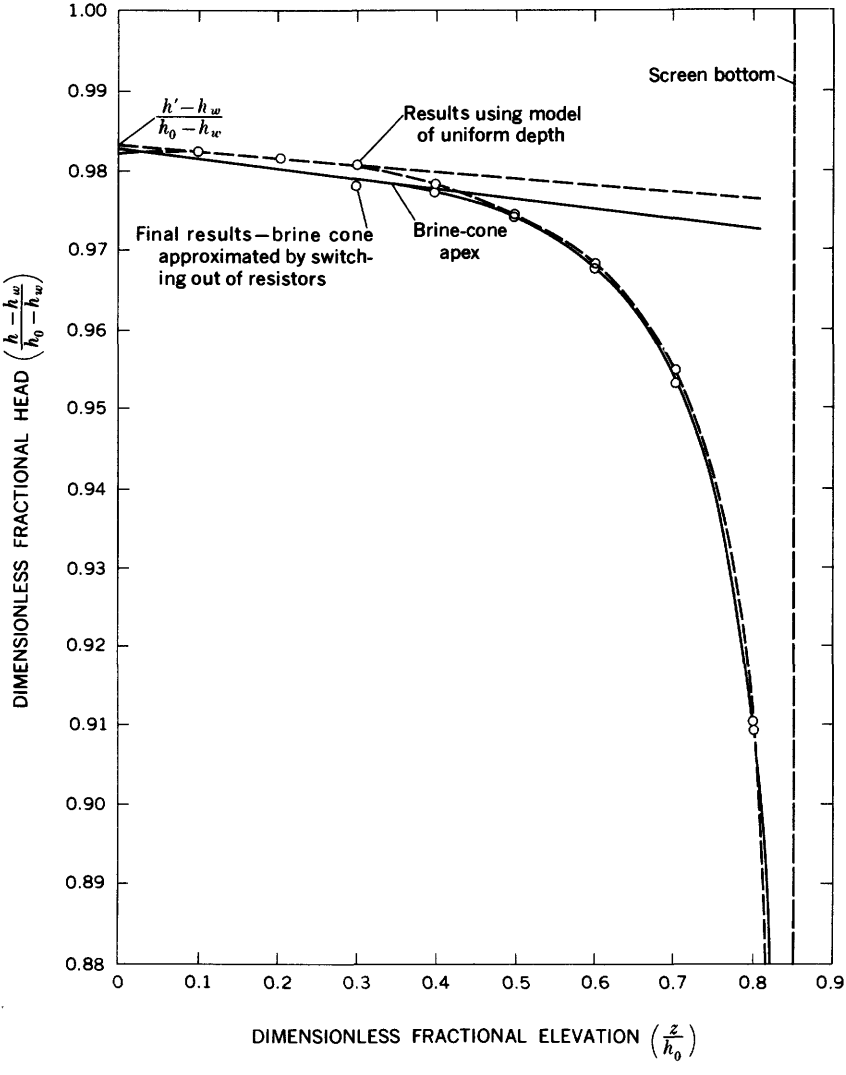

FIGURE 3.—Graph of $\frac{h-h_w}{h_0-h_w}$ versus $\frac{z}{h_0}$ at $\frac{r}{r_e}=\frac{r_w}{r_e}$, and tangent line, experiment A–6.

All the experimental results are approximation, inasmuch as the analog network yields only an approximate solution to the equation of flow. The elevations of the brine-cone apex should in particular be treated as approximate, as it was frequently difficult, in carrying out the graphical procedure, to fix the exact location of the point of tangency.

For a given density contrast and original thickness of fresh water, the inverse of the slope of the tangent line indicates the maximum permissible drawdown for operation of the well with no inflow of brine. This inverse slope, or maximum permissible drawdown function, has been plotted versus the fractional elevation of the screen bottom, $\frac{z_b}{h_0}$, for the three values of the flownet constant, in figure 7. It should be kept in mind that the maximum permissible drawdown, as taken from the experimental results, can be applied to a particular well only

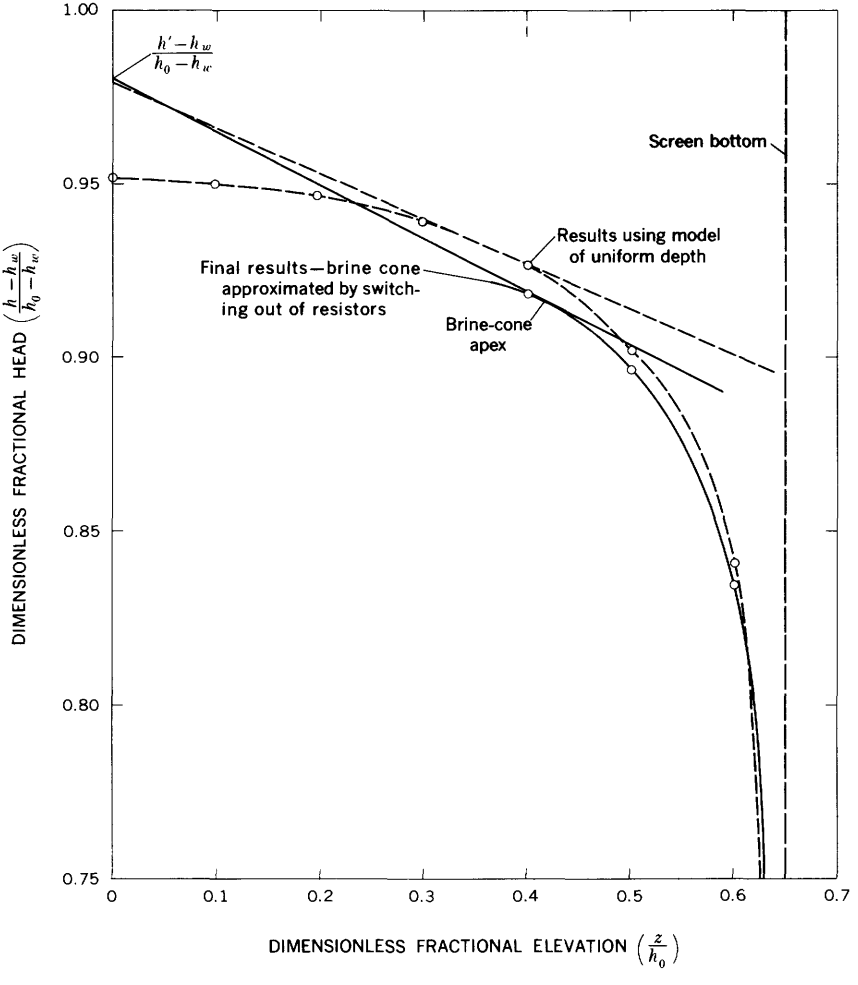

FIGURE 4.—Graph of $\frac{h-h_w}{h_0-h_w}$ versus $\frac{z}{h_0}$ at $\frac{r}{r_e}=\frac{r_w}{r_e}$, and tangent line, experiment B–4.

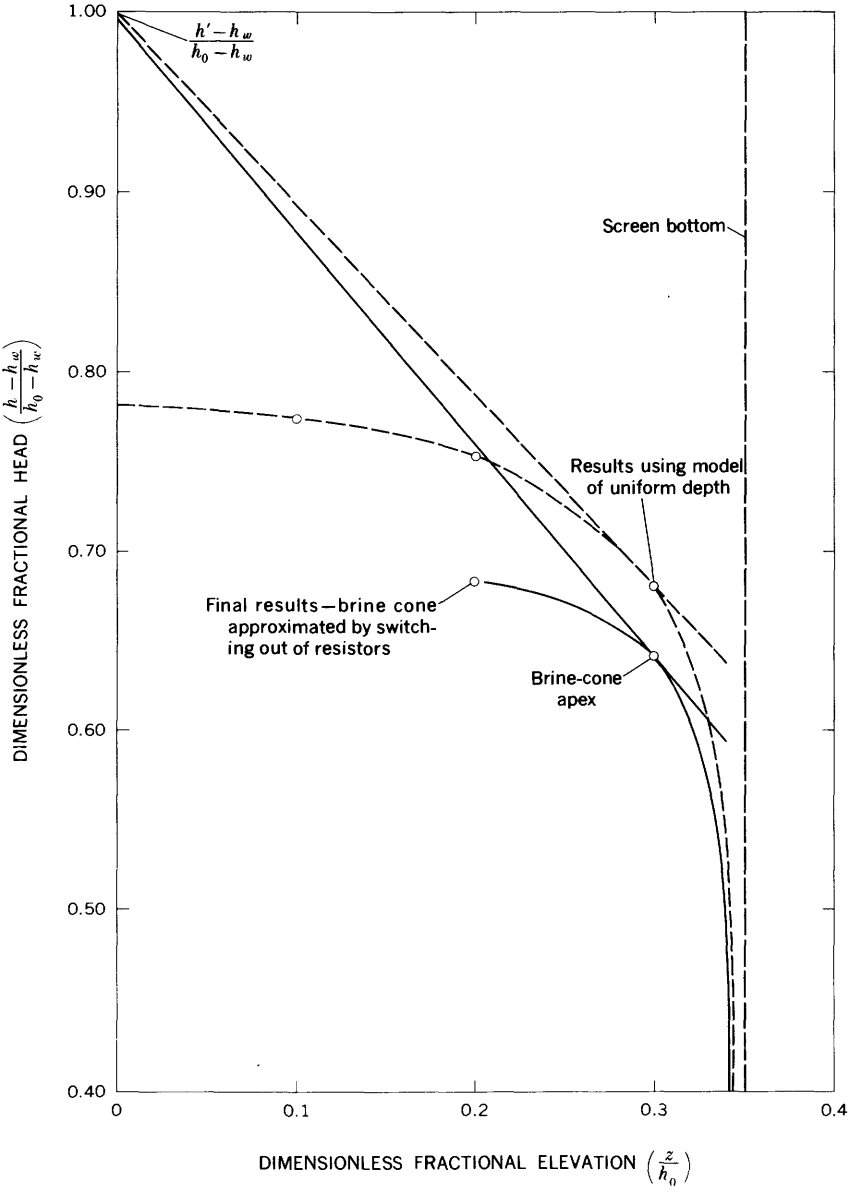

FIGURE 5.—Graph of $\frac{h-h_w}{h_0-h_w}$ versus $\frac{z}{h_0}$ at $\frac{r}{r_e}=\frac{r_w}{r_e}$, and tangent line, experiment C–1.

insofar as this drawdown is compatible with the construction of the well. A drawdown below the bottom of the well screen, for example, is clearly impossible; in most cases, moreover, a drawdown below the top of the screen is regarded as undesirable for various engineering reasons. Moreover, the analog model becomes a progressively less accurate representation of the flow system as the water level in the well falls below the top of the screen. Thus, in general, the maximum permissible drawdown from the experimental results should be applied in a given situation only if it represents a water level above the top of the screen. Otherwise, the level of the screen top should probably be taken as the minimum permissible water level in the well.

These conditions lead to the further conclusion that it may not be possible, in a given situation, to achieve the condition of maximum coning illustrated in the flownets. If, according to the maximum permissible drawdown function, $\frac{\rho_f(h_0-h_w)}{\Delta\rho h_0}$, associated with this condition of maximum coning, and the density contrast observed in the field, the drawdown associated with maximum coning turns out to be below the bottom of the well screen, maximum coning can never be achieved. In such a situation, the brine cone will stabilize at a lower position, associated with the drawdown that can actually be maintained in the well. To approach this aspect of the problem in another way, one may assign any practical drawdown limit (expressed as a fraction of h_0) on the basis of well construction, and then calculate the density contrasts, $\frac{\Delta\rho}{\Delta\rho_f}$, which would be required for maximum coning to occur at this practical limit of drawdown, from the data of figure 7. If the density contrast observed in the field exceeds this calculated value, the brine cone can never reach the highest stable position. If the density contrast is less than this calculated value, maximum coning will occur at a drawdown which is less than the practical limit; in this case, the drawdown at which maximum coning will occur may actually be taken as the limiting drawdown. In using the results quoted in this report, it might be reasonable to consider the distance from the static water table to the top of the screen, which was always 0.05 h_0, as the practical limit of drawdown. If this is done in the case of, say, a well screened from $\frac{z}{h_0}=0.95$ to $\frac{z}{h_0}=0.65$, in an aquifer in which $\left(\frac{h_0}{r_e}\right)^2\frac{K_l}{K_z}=0.423$, it is found that a condition of maximum stable coning can be achieved if $\frac{\Delta\rho}{\rho_f}$ is approximately 0.008, or less. At higher values of the density contrast, the water level will

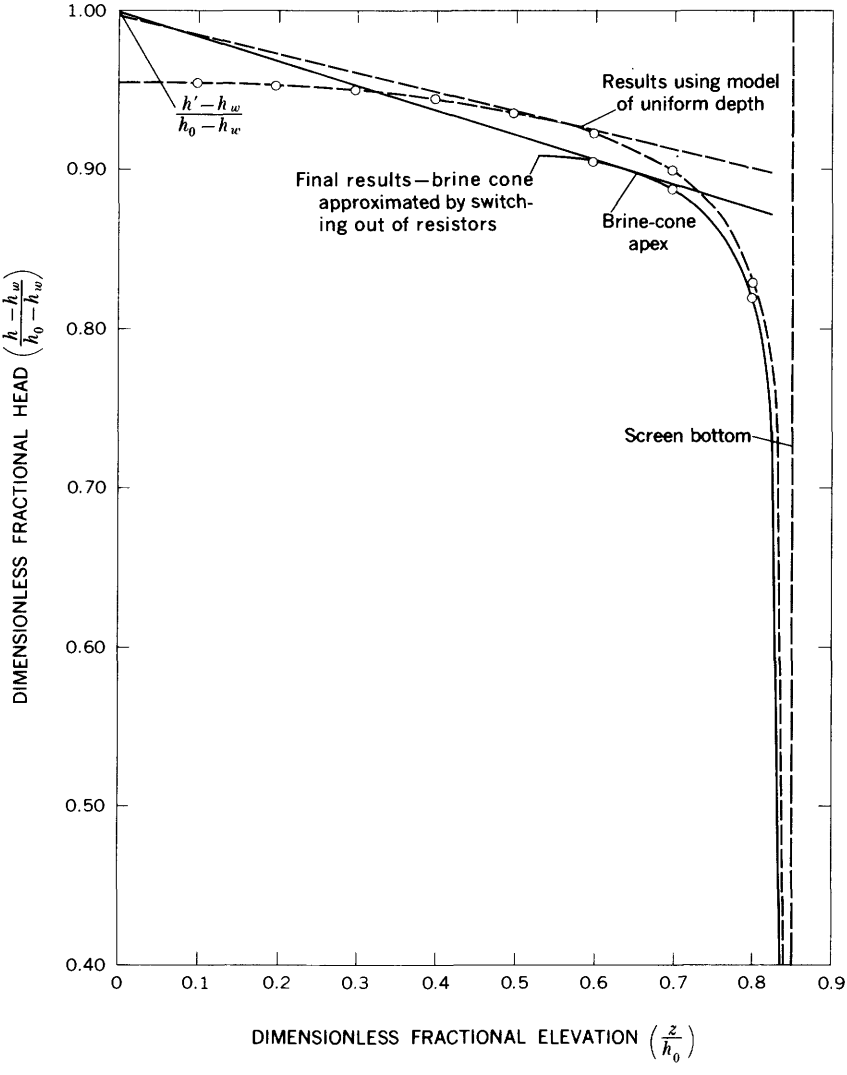

FIGURE 6.—Graph of $\frac{h-h_w}{h_0-h_w}$ versus $\frac{z}{h_0}$ at $\frac{r}{r_e}=\frac{r_w}{r_e}$, and tangent line, experiment C–6.

reach the top of the screen before the drawdown required for maximum coning is attained.

In figure 8 the dimensionless specific-capacity function has been plotted versus the fractional elevation of the screen bottom, again for the three values of the flownet constant. The product of the maximum permissible drawdown function and the dimensionless specific-capacity function indicates, for a given density contrast, original thickness of

fresh water, and lateral permeability, the maximum permissible discharge at which the well can operate without inflow of brine. This product, $\frac{Q\rho_f}{K_l h_0^2 \Delta\rho}$, has been designated the maximum permissible discharge function and plotted versus the elevation of the screen botton, for the three values of the flownet constant, in figure 9.

Each of the three curves of figure 9 shows a maximum at approximately $\frac{z_b}{h_0}=0.85$, indicating that with the screen top at $\frac{z}{h_0}=0.95$, and assuming the other conditions simulated in the experiments, the maximum discharge of uncontaminated fresh water is obtaintd with the screen bottom at $\frac{z}{h_0}=0.85$. It should be noted, however, that these maxima were calculated on the basis of extrapolated data; with the vertical network spacing of 0.1 h_0 and the screen top at 0.95, it was not possible to model a shorter screen than that used in experiments A–6, B–6, and C–6. The positions of the maxima should therefore be

TABLE 1.—*Results of the brine-coning experiments and graphical analyses*

[In all experiments the screen top was placed at $\frac{z}{h_0}=0.95$, and the ratio of r_w to r_e was 1 to 2,896]

Experiment	Flownet constant $\left(\frac{h_0}{r_e}\right)^2 \frac{K_l}{K_z}$	Screen bottom $\frac{z_b}{h_0}$	Apex of brine cone $\frac{z_a}{h_0}$	Slope of tangent line $\frac{\Delta\rho}{\rho_f}\cdot\frac{h_0}{h_0-h_w}$	Intercept of tangent line $\frac{h'-h_w}{h_0-h_w}$	Dimensionless specific-capacity function $\frac{Q}{h_0 K_l(h_0-h_w)}$
A–1	1. 71	0. 35	0. 22	0. 249	0. 885	0. 487
2	1. 71	. 45	. 26	. 145	. 909	. 419
3	1. 71	. 55	. 28	. 0814	. 929	. 343
4	1. 71	. 65	. 31	. 0500	. 949	. 267
5	1. 71	. 75	. 33	. 0275	. 967	. 187
6	1. 71	. 85	. 35	. 0125	. 983	. 101
B–1	. 423	. 35	. 30	. 610	. 963	. 532
2	. 423	. 45	. 32	. 365	. 967	. 452
3	. 423	. 55	. 39	. 247	. 973	. 372
4	. 423	. 65	. 41	. 154	. 980	. 290
5	. 423	. 75	. 47	. 0940	. 985	. 206
6	. 423	. 85	. 50	. 0460	. 993	. 114
C–1	. 0256	. 35	. 31	1. 198	. 997	. 583
2	. 0256	. 45	. 39	. 832	. 998	. 507
3	. 0256	. 55	. 47	. 600	. 998	. 428
4	. 0256	. 65	. 52	. 407	. 998	. 342
5	. 0256	. 75	. 61	. 277	. 999	. 247
6	. 0256	. 85	. 64	. 155	. 999	. 143

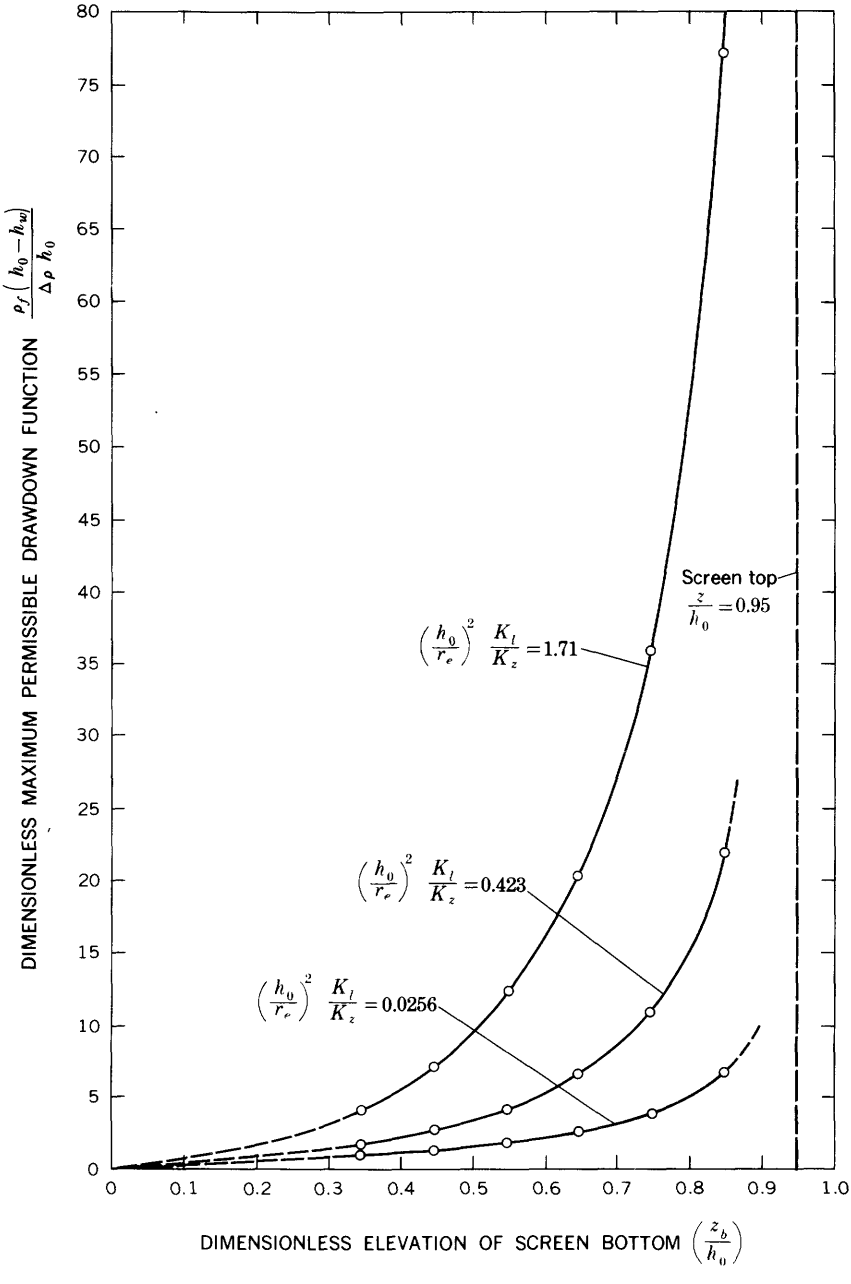

FIGURE 7.—Graphs of maximum permissible drawdown function, $\frac{\rho_f(h_0-h_w)}{\Delta\rho h_0}$, versus elevation of screen bottom, $\frac{z_b}{h_0}$.

considered only approximate. It should be noted, further, that the position of the screen bottom for which the maximum discharge of fresh water is possible, may not necessarily be the optimum operating position. If the requirements for fresh water are less than the maximum discharge which could be obtained with the screen bottom at 0.85, the required discharge could be pumped more economically from a longer screen, because of the higher specific capacity associated with greater screen lengths. Again, since the system must operate at equilibrium

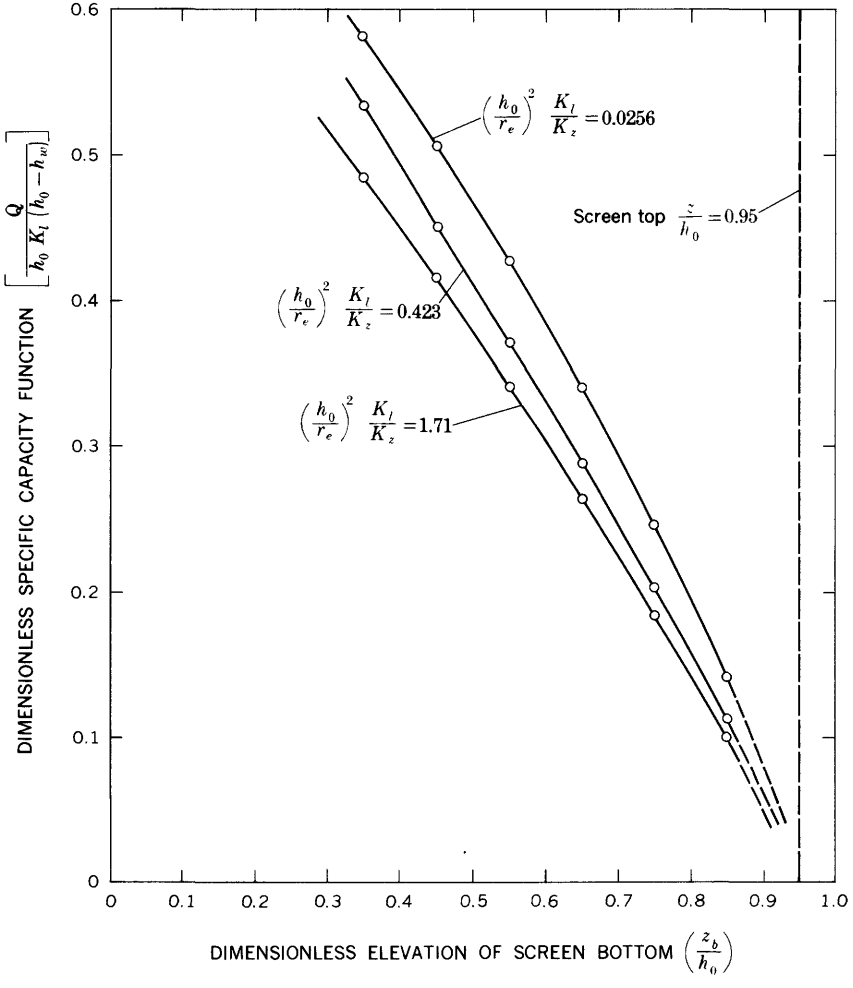

FIGURE 8.—Graphs of dimensionless specific-capacity function, $\frac{Q}{h_0 K_l (h_0 - h_w)}$, versus elevation of screen bottom, $\frac{z_b}{h_0}$, for conditions of maximum stable coning.

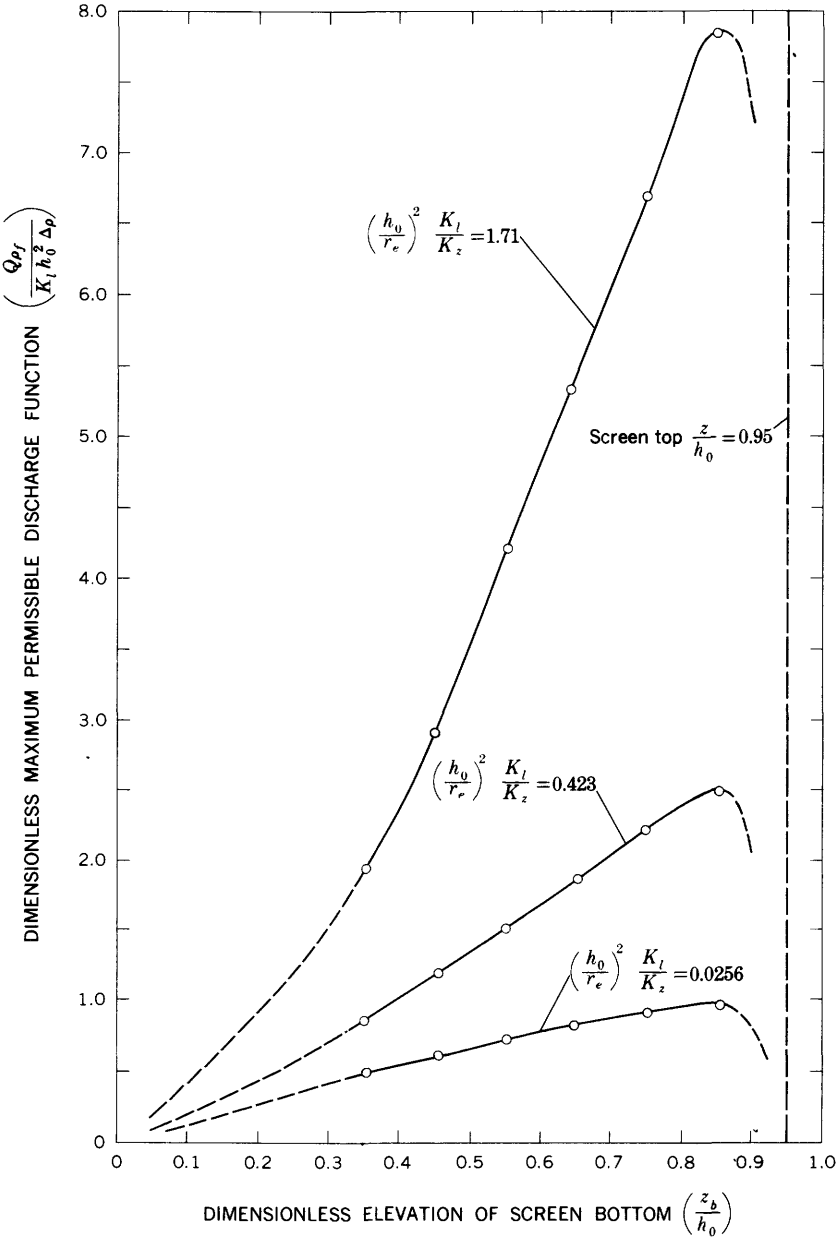

FIGURE 9.—Graphs of maximum permissible discharge function, $\frac{Q\rho_f}{K_l h_0^2 \Delta\rho}$, versus elevation of screen bottom, $\frac{z_b}{h_0}$.

for a stable brine cone to exist, the discharge may also be limited by the recharge available within the radius of influence. If this available recharge is less than the maximum permissible discharge with the screen bottom at 0.85, pumpage must be limited to balance the available recharge, and a longer screen may, therefore, again be used to gain economy of operation. This aspect of the problem may be viewed in a slightly different way if the well is relatively isolated from other wells, surface recharge is plentiful, and it is assumed that the radius of influence will ultimately stabilize when it has encompassed sufficient recharge to sustain the well discharge. Under these assumptions the value of r_e, and hence the value of the flownet constant, $\left(\frac{h_0}{r_e}\right)^2 \frac{K_l}{K_z}$, will depend upon the discharge at which the well is to be pumped. With the flownet constant thus determined, the screen bottom can be set at the deepest position at which the required discharge can be achieved without inflow of brine.

If construction and operation of a well field, rather than of a single well, are under consideration, the flownet constant, $\left(\frac{h_0}{r_e}\right)^2 \frac{K_l}{K_z}$, can be considered a variable over which some control is possible, in the sense that the radius of influence, r_e, depends upon the well spacing in the interior of a well field. It is interesting, therefore, to plot the maximum permissible drawdown function, $\frac{\rho_f(h_0-h_w)}{\Delta\rho h_0}$, the dimensionless specific-capacity function, $\frac{Q}{h_0 K_l(h_0-h_w)}$, and the maximum permissible discharge function $\frac{Q\rho_f}{K_l h_0^2 \Delta\rho}$, versus the flownet constant, $\left(\frac{h_0}{r_e}\right)^2 \frac{K_l}{K_z}$. These plots are shown in figures 10–12, respectively, each of which shows six graphs, corresponding to the six positions of the screen bottom used in the experiments. Over the range of flownet-constant values represented in the experiments, the maximum permissible drawdown (fig. 10) and the maximum permissible discharge (fig. 12), appear to be approximately linear functions of the flownet constant. In the operation of a well field at equilibrium, maximum utilization of the available recharge is attained if the spacing and discharge of the wells are such as to satisfy the equation

$$Q = W\pi r_e^2, \tag{11}$$

where W is the rate of recharge per unit area, and r_e may be taken, approximately, as half the well spacing. For a given set of field conditions—that is, for given values of $\Delta\rho$, ρ_f, K_l, K_z, h_0, and W—algebraic

or graphic combination of equation 11 with the relations indicated in figures 10–12 may be used to indicate the optimum practical depth and spacing of wells in the field.

EXAMPLES OF CALCULATIONS APPLICABLE TO THE PUNJAB REGION

Extensive trial calculations are beyond the scope of this paper. Very little calculation is required, however, to demonstrate that prospects are encouraging in the Punjab Region for the development

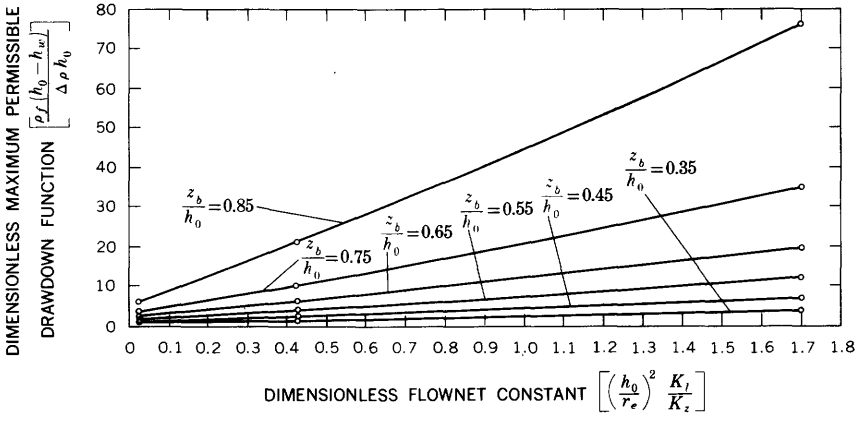

FIGURE 10.—Maximum permissible drawdown function, $\frac{\rho_f(h_0-h_w)}{\Delta\rho h_0}$, versus flownet constant, $\left(\frac{h_0}{r_e}\right)^2\frac{K_l}{K_z}$, for various positions of the screen bottom.

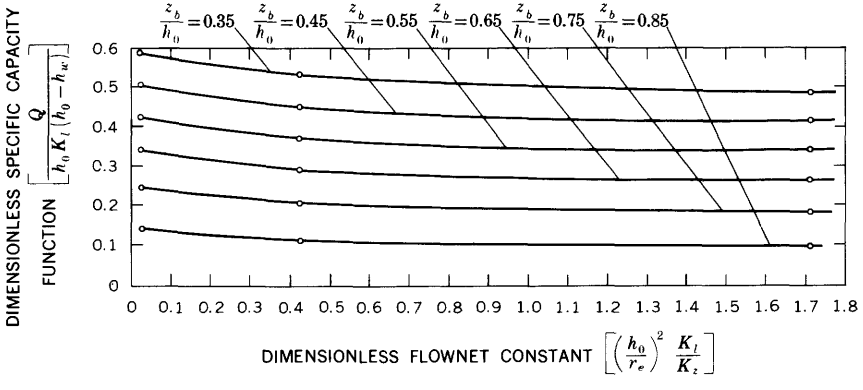

FIGURE 11.—Dimensionless specific-capacity function, $\frac{Q}{h_0K_l(h_0-h_w)}$, versus flownet constant, $\left(\frac{h_0}{r_e}\right)^2\frac{K_l}{K_z}$, for various positions of the screen bottom.

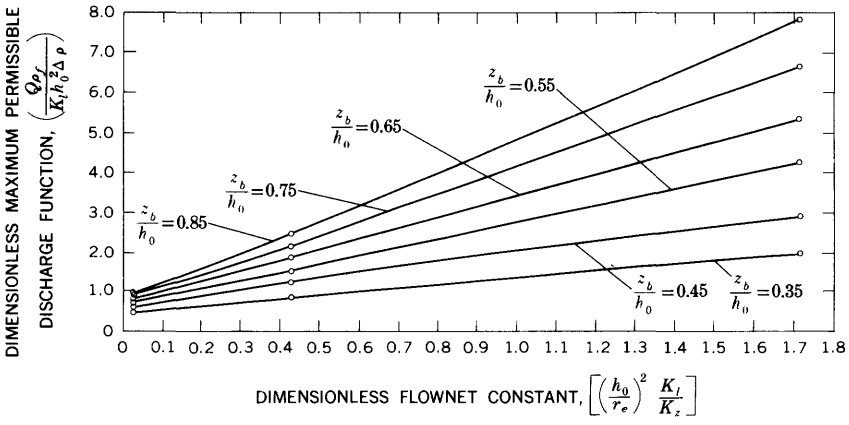

FIGURE 12.—Maximum permissible discharge function, $\frac{Q\rho_f}{K_l h_0^2 \Delta\rho}$, versus flownet constant, $\left(\frac{h_0}{r_e}\right)^2 \frac{K_l}{K_z}$, for various positions of the screen bottom.

of wells that can discharge fresh water above a static cone in an underlying layer of poor-quality water. Suppose, for example, we consider an area in which the original thickness of fresh water is 100 feet, the lateral permeability is 0.002 cfs per sq ft (cubic feet per second per square foot), the anisotropy ratio, $\frac{K_l}{K_z}$, is 10, and the density contrast, $\frac{\Delta\rho}{\rho_f}$, between fresh water and underlying saline water is 0.02. Suppose further, that we wish to study the performance of wells 0.7 foot in radius, screened from 5 to 35 feet below the water table, and spaced about 4,000 feet apart in a field. The flownet constant applicable to this problem wlll be $\left(\frac{h_0}{r_e}\right)^2 \frac{K_l}{K_z}=0.025$, if we consider r_e to be one-half the distance between wells; and, to a close approximation, the results of experiment C–4 may be applied. Using these results, the drawdown corresponding to maximum stable coning is calculated as 4.9 feet, whereas the discharge at this drawdown is approximately 0.34 cfs. The top of the well screen is at a depth of 5 feet below the static water table in this case, so that if entrance losses are negligible, it should be possible to achieve the condition of maximum stable coning. The required intensity of recharge for equilibrium operation at this discharge and spacing would be about 0.75 cfs per sq mi. As this is somewhat less than the recharge apparently available in the Punjab Region (Mundorff and Lateef, 1964), it is probable that the optimum type of development for the conditions used in this example would incorporate wells of somewhat closer spacing than 4,000 feet.

The above example relates primarily to the skimming-well problem—that is, to the problem of pumping from a thin layer of fresh water, where the underlying brine is of relatively high density. To illustrate the implications of the results for conventional project development, we may take an example in which the original thickness of fresh water is 500 feet, the anisotropy, $\frac{K_l}{K_z}$, is 14, the lateral permeability is 0.002 cfs per sq ft, the density contrast, $\frac{\Delta\rho}{\rho_f}$, is 0.01, and we are interested in the performance of wells 1 foot in radius, screened from 25 to 175 feet below the water table, and spaced 5,800 feet apart. The flownet constant for this problem, again taking r_e as one-half the spacing, is approximately 0.42, and the results of experiment B–4 may be used to represent the problem. The maximum permissible drawdown calculated from the experimental results for these conditions is 32.5 feet. As the top of the screen is 25 feet below the water table in this case, the condition of maximum stable coning might never be reached. If the dimensionless specific-capacity figure from experiment B–4 is used to calculate the discharge corresponding to 25 feet of drawdown for this well, a figure of 7 cfs is obtained. Use of this dimensionless specific capacity in this way is not strictly correct, since the specific-capacity figures obtained in the experiments correspond to the condition of maximum stable coning, while in this example the cone is below the highest possible stable position when the drawdown in the well is 25 feet. The error due to this approximation is probably slight, however, as a small change in the position of the interface should not greatly affect the specific capacity. The figure of 7 cfs for 25 feet of drawdown neglects all entrance loss, and for this reason is certainly too high. Even allowing for entrance loss, however, it is probable that at least 4 cfs could be pumped with the water level at the top of the screen; the drawdown on the outer surface of the screen would then be much less than 32.5 feet, and the brine cone would stabilize below the highest possible position. In any case, there would seem to be little chance of contamination of the well by poor-quality water in this example, assuming that recharge were sufficient to sustain equilibrium operation.

The use of a well radius of 1 foot in the above trial calculation is perhaps unrealistic, and probably causes the result to be optimistic. As the ratio of r_w to r_e was fixed by construction of the model, to assume a value for either r_w or r_e in a trial calculation is to fix the other. This difficulty can be circumvented to a certain extent by assuming that a change in r_w will extend or reduce the lateral portions of the flowliness, near the screen, causing reduction or increase in the specific capacity of the well, but will not otherwise affect the flow

pattern. In the preceding example we might utilize this assumption by considering 1 foot to be the radius of the gravel pack rather than of the screen. The maximum permissible drawdown calculated using figure 7 would then refer to drawdown at the edge of the gravel pack; to this, we would have to add the drawdown through the gravel pack and, for a full representation of the problem, the entrance losses of the well. The specific capacity as taken from figure 8 would in this case represent the ratio of the well discharge to drawdown at the edge of the gravel pack; the actual specific capacity of the well could be calculated from this figure, taking into consideration the additional drawdown through the gravel pack and screen. Finally, the maximum permissible discharge, as taken from figure 9 or 10, could be corrected in the same way. In applying this type of adjustment to deal with different ratios of r_w to r_e, it is of course unnecessary to assume that the experimental results apply at the edge of the gravel pack. They may be assumed to apply at any radius, so long as the fundamental assumption is satisfied, that within this radius changes in r_w only alter the length of the horizontal portion of the flowlines, and otherwise do not alter the flow pattern.

CONCLUSIONS

The analog technique, coupled with Muskat's graphical procedure, provides a convenient way of studying the problem of brine coning beneath a fresh-water well. The results herein presented may be applied to problems in which the flownet constant and screen penetration fall within the ranges covered in the experiments, and in which the decrease in thickness of flow due to drawdown of the free surface is much less than the decrease in thickness of flow due to brine coning. Within the range of conditions represented in the experiments, and with the screen top at $\frac{z}{h_0}=0.95$, the results indicate that the maximum discharge of fresh water over a stable brine cone can be obtained by placing the screen bottom approximately $\frac{z}{h_0}=0.85$. However, this may not be the optimum position in terms of economics of pumping in a given case. As the flownet constant, $\left(\frac{h_0}{r_e}\right)^2 \frac{K_l}{K_z}$ increases, there is an approximately linear increase in the maximum permissible drawdown and in the maximum permissible discharge, within the range of flownet constants from 0.0256 to 1.71.

Applied to conditions in the Punjab, the results indicate that there are good prospects for the development of wells capable of discharging fresh water above a static cone in the underlying brine or brackish water. In areas where the original thickness of fresh water is ap-

preciable, say 500 feet or more, there should be little danger of serious contamination in reclamation projects of the type presently under development in the Punjab. Where the thickness of fresh water is less, contamination can probably be avoided by careful planning and controlled operation. The concept of shallow skimming wells does not appear to be unreasonable for areas where the layer of fresh water is thin.

This paper represents a preliminary effort to deal with the problem of brine coning beneath fresh-water wells, using analog techniques. Much additional work is needed. Studies covering a wider range of flownet constants are particularly needed, as are studies incorporating different positions of the screen top, different ratios of r_w to r_e, and screen penetrations shallower than $\frac{z}{h_0}=0.85$. A further need is the study of heterogeneous systems, in particular those in which a low permeability layer occurs between the bottom of the screen and the brine interface.

The experimental results serve to reemphasize the point made by Muskat, that there is a certain highest stable position for the brine cone in every case, above which brine cannot occur under static conditions. This highest stable position, as described in terms of the dimensionless coordinates $\frac{z}{h_0}$ and $\frac{r}{r_e}$, is a function of the flownet constant and the boundary conditions, in particular, the fractional elevation of the screen top and screen bottom, $\left(\frac{z_b}{h_0}, \frac{z_t}{h_0}\right)$ and the fractional screen radius $\left(\frac{r_w}{r_e}\right)$. The highest stable position is the same regardless of the density contrast, although the drawdown and fresh-water discharge associated with the highest stable-cone position increase as the density increases. The apex of the highest stable cone is always some distance below the bottom of the screen, and the head at this apex point is always much higher than the head at the well screen itself; analyses which neglect this point, by assuming that the head at the apex of the brine cone is equal to the head at the screen, and that maximum uncontaminated discharge occurs with the apex of the brine cone just at the base of the screen, must yield erroneous results.

The calculations presented in this paper serve to indicate the conditions under which stable coning can be achieved. It is by no means the authors' intention to propose that a condition of stable coning should always be the objective, when pumping from an aquifer in which fresh water is underlain by brine. In many instances it may

be preferable to allow brine to enter the well, if the salinity of the pumped mixture is within tolerable limits, and particularly if conditions suggest that this type of operation may lead to a progressive improvement in water quality within the aquifer. The decision as to whether or not to attempt the development of a stable brine cone in a particular case is an engineering or water-management decision, which should be based upon full consideration of all aspects of the local water situation.

REFERENCES CITED

Hubbert, M. K., 1940, The theory of ground-water motion: Jour. Geology v. 48, no. 8, pt. 1.

Mundorff, M. J., and Lateef, M. A., 1963, Relation of ground water withdrawal and the decline in the water table, SCARP 1, Rechna Doab: Water and Soils Inv. Div. Tech. Paper No. 5.

Muskat, Morris, 1937, The flow of homogeneous fluids through porous media: repr., 1946, Ann Arbor, Mich., J. W. Edwards, Inc., p. 487–490.

——— 1949, Physical principles of oil production: New York, McGraw Hill Co., p. 226–236.

Stallman, R. W., 1963, Electric analog of three-dimensional flow to wells and its application to unconfined aquifers: U.S. Geol. Survey Water-Supply Paper 1536–H.

U.S. GOVERNMENT PRINTING OFFICE : 1968—O-306-887